Assessment of miniature Knowles sensor for the measurement of wall pressure fluctuations

Nan Hu

German Aerospace Center (DLR), Institute of Aerodynamics and Flow Technology, Department of Technical Acoustic, Email: nan.hu@dlr.de

Introduction

The wall pressure fluctuations can be measured using a flush-mounted or a pinhole-mounted sensor construction. Due to signal averaging over the sensor surface [1], a small sensing area is required to minimize the high-frequency spectral attenuation. The pinhole-mounted construction is an effective means to reduce the sensing area. However, even for the pinhole-mounted construction, a miniature pressure sensor is needed to increase the resonance frequency of the pinhole construction.

In the present work, two Knowles miniature sensors, model FG-23329-P07, along with Kulite miniature sensors were mounted on a flat plate model for measurement in the Acoustic Wind Tunnel Braunschweig (AWB). Both sensor types were pinhole mounted with a pinhole diameter of 0.5 mm. The wall pressure fluctuations were measured in zero pressure gradients (ZPG) for various flow velocities and also in adverse and favorable pressure gradients (APG, FPG). The mean flow velocities across the boundary layer were obtained using a single-wire hot-wire probe. The one- and two-point statistics of the wall pressure fluctuations measured by the Knowles sensors are analyzed and compared to those measured by the Kulite sensors. Based on the comparison, the performance of the Knowles sensors for the measurement of wall pressure fluctuations is assessed.

Experimental setup

The experiment was conducted in the open-jet anechoic test section of AWB. The wind tunnel has a rectangular nozzle with a height of 1200 mm and a width of 800 mm. The maximum operating velocity is 65 m/s. A photograph of the experimental setup is shown in Fig. 1. A flat wooden plate was placed 10 mm downstream of the nozzle exit at the mid-height nozzle position. The plate surface was aligned with the flow direction. The length and thickness of the plate are 1350 mm and 42 mm, respectively. The plate span is 1300 mm, which is 250 mm wider than the nozzle exit on each side to prevent side-edge interaction with the tunnel jet shear layers. A 125 mm long super-elliptically shaped leading edge was selected to avoid flow separation [2]. Both sides of the plate were tripped at 120 mm behind the leading edge tip with 0.3 mm zigzag strips. A 12° beveled trailing edge on the underside of the plate was used to realize a ZPG turbulent boundary-layer on the top side in the rear area [3]. The trailing-edge tip was extended by foam serrations to minimize vortex shedding and to reduce trailing-edge noise.

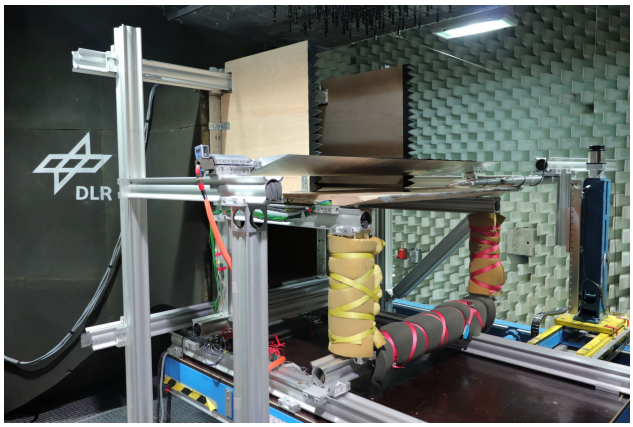

Figure 1: Photograph of the experimental setup.

Pressure gradients were produced by placing a NACA 0012 airfoil with 400 mm chord length and 1800 mm span width above the plate. The airfoil with its leading edge at $x = 760$ mm was installed 120 mm above the plate relative to the wing's chord at the geometric angle of attack (AOA) of 0°. Both sides of the airfoil were tripped at 20% chord length with 0.4 mm zigzag strips and a trailing-edge brush with an extent of 920 mm was utilized. The axis of rotation was at 41% of the chord length. The AOA of the airfoil was varied between -14° and 14° to produce the desired flow conditions. Furthermore, the nozzle exit above the plate was extended by wooden sidewalls with foam-serration trailing-edge extensions to reduce the tunnel jet shear-layer impact on the measured wall pressure spectra.

A 370 mm long, 270 mm wide and 5 mm thick aluminum panel, equipped with 26 static pressure ports and different types of dynamic pressure sensors, was placed at mid-span in the rear portion of the plate. The static pressure was recorded in the streamwise direction between 930 mm $\leq x \leq$ 1220 mm (x=0 denotes the leading edge of the plate) and spanwise direction between $|z| \leq 90$ mm ($z = 0$ denotes the mid span of the plate). The wall pressure fluctuations were measured in a range of 1105 mm $\leq x \leq$ 1210 mm with various types of Kulite sensors, 1/4" and 1/8" Microphones, and a pair of Knowles sensors. In the present work, signals measured by a Knowles sensor pair (model FG-23329-P07, a diameter of 2.6 mm) were compared with those measured by a Kulite sensor pair (model LQ-062-0.35bar, a diameter of 1.6 mm without the protection screen). The sensor pairs were located at the same streamwise posi-

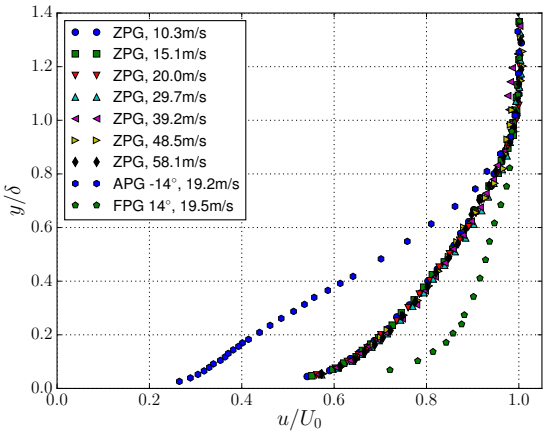

Figure 2: Boundary layer profiles at $x = 1170$ mm, $z = 0$ mm.

tions, $x = 1165, 1170$ mm, with a spanwise separation of $\Delta z = 41$ mm (the Kulite sensors at $z = 0$). All the selected sensors were pinhole mounted with a pinhole diameter of 0.5 mm and a depth of 0.4 mm. During the measurement, the sampling rate was set at 100 kHz and the data were recorded for 30 s. A preamplifier with a gain factor of 250 and a first-order high pass filter with a cut-off frequency at 270 Hz was applied for the Kulite sensor. The power spectra measured by the Kulite sensor shown in this paper are corrected using the filter frequency response curve.

Flow velocity within the boundary layer was measured using a single-wire hot-wire probe. The hot-wire data were recorded for 10.3 s with a sampling rate of 50 kHz and a low pass filter of 20 kHz.

Results

Mean flow statistics

The mean flow velocity for different flow conditions was measured at $x = 1170$ mm, $z = 0$ mm. Fig. 2 shows the measured boundary layer profiles normalized with the boundary layer thickness δ and the local free-stream velocity U_0 for different velocities in ZPG flows and selected cases in APG and FPG flows. The ZPG profiles for different velocities fall together. The normalized velocity for the APG flow is smaller than the ZPG flow at $y/\delta < 0.8$, whereas for the FPG flow is larger. This trend agrees well with the experimental results from the literature [4, 5].

Some relevant boundary layer parameters are summarized in Table 1. To determine the boundary layer displacement thickness δ^*, the mean velocities for locations $y < 1$ mm (not measured) are estimated using the Spalding's wall law [6]. The value of shape factor H for the ZPG flows decreases as the flow velocity and the Reynolds number increase. Chauhan *et al.* [7] collected an extensive experimental dataset for ZPG flows and show that, H falls approximately from 1.43 to 1.35 as Re_θ increases from 2000 to 9000. Compared to the results from the literature, the obtained values of H from the current measurement are slightly larger, which is probably due to a weak APG, $dCp/dx < 0.15$ m^{-1}(not shown), measured in the plate rear region between 930 mm $\leq x \leq$ 1220 mm.

	U_0 (m/s)	δ (mm)	δ^* (mm)	$H = \delta^*/\theta$	$Re_\theta = U_0\theta/\nu$
ZPG	10.3	22.5	4.19	1.45	1978
	15.1	21.2	3.89	1.44	2718
	20.0	19.9	3.64	1.43	3387
	29.7	19.6	3.45	1.41	4831
	39.2	19.2	3.53	1.40	6612
	48.5	18.3	3.23	1.40	7437
	58.1	18.5	3.31	1.40	9180
APG -14°	19.2	38.3	12.19	1.97	7923
FPG 14°	19.5	14.6	1.54	1.31	1534

Table 1: Boundary layer parameters.

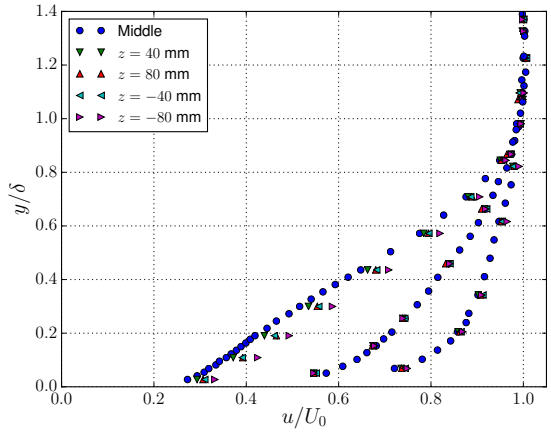

Figure 3: Boundary layer profiles at $x = 1170$ mm for different spanwise locations.

The two-dimensional (2-D) flow condition was checked by measuring the boundary layer profile at four different spanwise positions between $|z| \leq 80$ mm. Results shown in Fig. 3 verify the 2-D flow condition within the measured spanwise extent for the ZPG and FPG cases. However, due to the influence of the installed airfoil on the plate boundary layer, a slight difference in the boundary layer profiles between different positions were observed for the APG case. Note, that an uncertainty of ± 0.1 mm for the positioning of the first hot-wire measurement point is suggested. This uncertainty could cause a noticeable difference for the measured boundary layer profile in the near-wall region at the different spanwise positions.

Wall pressure one-point statistics

Firstly, a comparison of the frequency response of the Knowles and Kulite sensors was made by using two loudspeakers placed at 855 mm and 900 mm upstream of the sensor position before the sidewalls were installed. The measured power spectral density (PSD) shows a good agreement between both sensors up to 10 kHz, indicating the range of a linear frequency response for the Knowles sensor, see Fig. 4. Spectral levels in this paper are ref-

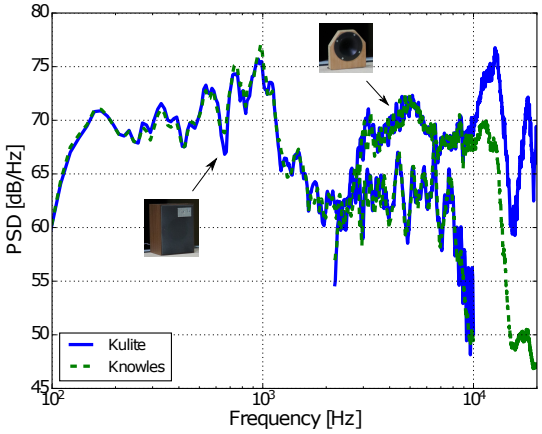

Figure 4: One-point spectra of loudspeaker signals.

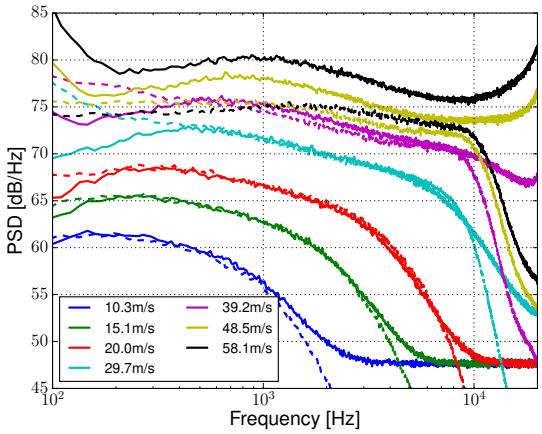

Figure 5: One-point spectra for the ZPG cases listed in Table 1. (–), Kulite; (- -), Knowles.

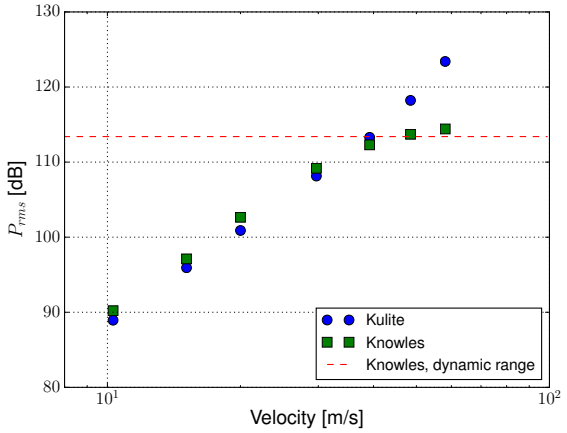

Figure 6: RMS value of the wall pressure fluctuations for the ZPG cases listed in Table 1.

erenced to a 20 μPa reference pressure. The spectra are calculated using a Hanning window with 8192 samples per window, and 50% overlap, resulting in a frequency resolution of 12.2 Hz.

Fig. 5 shows the measured wall pressure one-point spectra for ZPG boundary layers listed in Table 1. The spectra measured by the Kulite sensor agree well with the results from the literature [5]. The spectral level grows and the peak location shifts to a higher frequency as the flow velocity increases. At high velocities, i.e. 48.5 m/s and 58.1 m/s, the impacts of the low-frequency disturbance from the tunnel jet shear layer and the resonance of the pinhole construction at high frequencies on the measured spectra are clearly visible. Spectral levels below 48 dB are buried by the electrical noise.

The spectra measured by the Knowles sensor show good agreement with those measured by the Kulite sensor at low velocities ≤ 20 m/s, except for a small discrepancy at low frequencies. The low-frequency discrepancy grows as the velocity increases until 40 m/s. At the larger velocities, a distorted spectrum over the whole frequency range was measured and the spectral level does not change as the velocity further increases. In this work, the spectrum measured by the Kulite sensor is assumed to be correct. The discrepancy measured by both sensors is regarded as a distortion induced by the Knowles sensor.

The RMS value of the wall pressure fluctuations for the ZPG cases is plotted in Fig. 6. A low-pass filter is applied for the calculation of Kulite signals at low velocities to eliminate the influence of the electrical noise. The obtained values from the two sensors show good agreement up to a flow velocity of 40 m/s. At the larger velocities, the RMS value reaches the dynamic range of the Knowles sensor (estimated using a sinusoidal signal) and increases afterwards very slowly. The slightly smaller RMS value obtained by the Kulite sensor at lower velocities is caused by the applied high-pass filter. A significant low-frequency discrepancy was measured between both sensors at $U_0 = 29.7$ m/s, refer to Fig. 5, which indicates that a spectral distortion measured by the Knowles sensor occurs first at low frequencies and before the signal reaches the sensor's dynamic range. After reaching the dynamic range of the sensor, the spectral distortion can be observed over the whole frequency range.

The spectra measured by the Knowles and Kulite sensors for the APG and FPG cases at a low flow velocity show slight low-frequency discrepancies, see Fig. 7, which is comparable with the ZPG case.

Wall pressure two-point statistics

A comparison of the two-point statistics is accomplished by analyzing the signals measured by a sensor pair with a streamwise separation of 5 mm. The coherence is calculated using a Hanning window with 4096 samples per window, and 50% overlap, resulting in a frequency resolution of 24.4 Hz.

Fig. 8 shows the measured coherence for the ZPG flows at selected velocities. A smaller coherence value was measured at lower frequencies by the Knowles sensor. The loss of the coherence and the frequency range with the reduced coherence are larger with an increasing flow velocity. In contrast to the results for the one-point spectra, which show a spectral distortion over the whole frequency

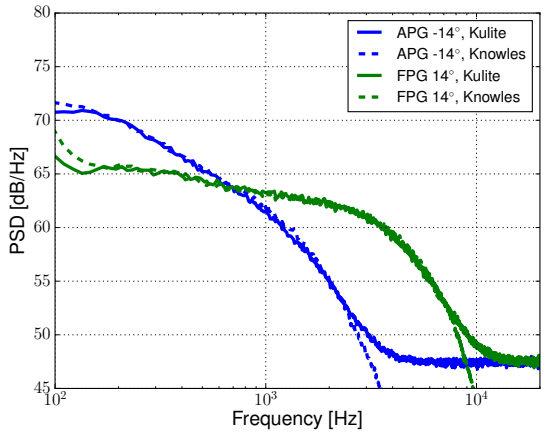

Figure 7: One-point spectra for the APG and FPG cases listed in Table 1.

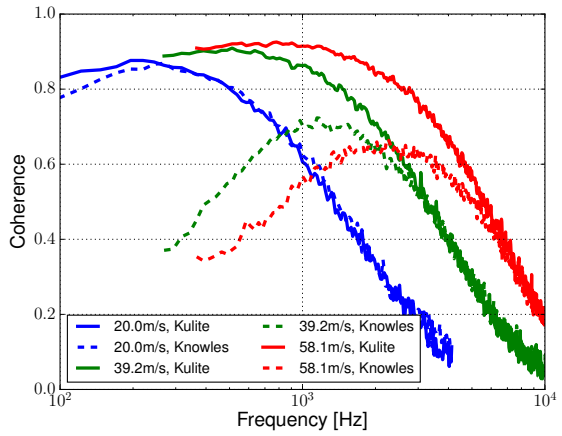

Figure 8: Coherence for a streamwise separation of 5 mm.

range at higher velocities, there is a good agreement between the output of both sensors at high frequencies.

Fig. 9 shows the convection phase velocity U_c, which is obtained through $U_c = \omega \Delta x / \theta$, where ω is the angular frequency, Δx is the streamwise separation between a sensor pair, and θ is the measured phase difference between them. Comparable to the results for the one-point spectra, a good agreement for the measured phase velocity between the Knowles and Kulite sensors is obtained at the lower flow velocity. As the flow velocity increases, a spectral distortion was measured by the Knowles sensor first at low frequencies, and the distortion can be observed over the whole frequency range for the largest test flow velocity.

Conclusion

The wall pressure fluctuations beneath turbulent boundary layers were measured at a flat plate model using pinhole-mounted Kulite and Knowles miniature sensors. A comparison of one- and two-point statistics of the measured wall pressure fluctuations between both sensors was made. The measured spectral discrepancy is regarded as a distortion induced by the Knowles sensor.

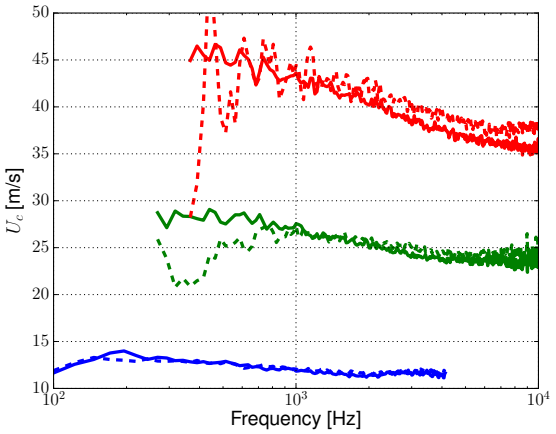

Figure 9: Phase velocity for a streamwise separation of 5 mm. Same legend as in Fig. 8.

The one-point spectra measured by the Knowles sensor show good agreement with those measured by the Kulite sensor at low flow velocities. As the velocity increases, a spectral distortion was measured by the Knowles sensor first at low frequencies. After the signal reaches the sensor's dynamic range at high velocities, the distortion can be observed over the whole frequency range.

In line with the observation made for the one-point spectra, consistent results for the coherence and the phase velocity were measured by a Knowles sensor pair at low flow velocities. As the flow velocity increases, the spectral distortion measured by Knowles sensor can be observed in a broader frequency range and with a larger level.

References

[1] Corcos, G. M.: Resolution of Pressure in turbulence, J. Acoust. Soc. Am., Vol. 35, pp. 192–199, 1964.

[2] Narasimha, R. and Prasad, S. N.: Leading edge shape for flat plate boundary layer studies, Experiments in Fluids, Vol. 17(5), pp. 358–360, 1994.

[3] Mosallem, M. M.: Numerical and experimental investigation of beveled trailing edge flow fields, Journal of Hydrodynamics, Vol. 20(3), pp. 273–279, 2008.

[4] White, F. M.: Viscous fluid flow, McGraw-Hill Inc., 1991.

[5] Hu, N. and Herr, M.: Characteristics of wall pressure fluctuations for a flat plate turbulent boundary layer with pressure gradients, AIAA Paper 2016-2749, 2016.

[6] Spalding, D. B.: A single formula for the law of the wall, J. Appl. Mech., Vol. 28, pp. 455–457, 1961.

[7] Chauhan, K. A., Monkewitz, P. A. and Nagib, H. M.: Criteria for assessing experiments in zero pressure gradient boundary layers, Flud Dyn. Res., vol. 41, pp. 021404, 2009.